Single Step Synthesis of Graphene Oxide Protected Silver Nanoparticles Using Aniline as Reducing Agent and Study its Application on Electrocatalytic Detection of Nitrite in Food Samples

Research Article

A. Sudarvizhi, Z. Ayesha Siddiqha and K. Pandian*

Department of Inorganic Chemistry, University of Madras, Guindy Campus, Chennai-600 025, India

*Corresponding author: K. Pandian, Department of Inorganic Chemistry, University of Madras, Guindy Campus, Chennai-600 025, India, Email: jeevapandian@yahoo.co.uk

Abstract

Silver nanoparticles (AgNP) decorated reduced graphene oxide was synthesized in a single step method using aniline as reducing agent. The electrochemical behavior of the silver nanoparticles modified graphene oxide was investigated and applied for the electrochemical oxidation of nitrite at different experimental conditions. An enhanced catalytic oxidation of nitrite was noted under optimum experimental condition using AgNP/RGO modified GCE which can be utilized for the electrocatalytic detection of nitrite in food samples. The detection limit for nitrite in the above range was found to be 2.6×10^{-7} M.

Keywords: Silver nanoparticles, Graphene oxide, Aniline, Detection of Nitrite, Food Samples

Introduction

Nitrite (NO_2^-) has been widely exploited in our daily life as food additives, excessively disposed into the ecosystem, and recognized as an alarming pollutant to the environment and human health. In ecosystem NO_2^- is of interest because of its toxicity for microorganisms and higher organisms [1] The World Health Organization has reported that the fatal dose of nitrite ingestion is between 8.7 μM and 28.3 μM [2]. It is a major oxidation product derived from NO that is produced in a wide variety of cell types by NO synthases [3]. Moreover, NO_2^- accumulated in the human body may cause methemoglobinemia and furthermore, may become source of carcinogenic N-nitrosamines [4,5]. As a consequence, accurate, rapid and economic determination of NO_2^- has attracted much attention. Many methods have been developed to detect nitrite, such as electrochemical biosensors [6, 7], spectrophotometry [8, 9], gas chromatography-mass spectrometry [10], ion chromatography [11], spectrofluorimetry [12, 13], chemiluminescence [14], flow injection analysis [15] and capillary electrophoresis [16]. Among these methods, electrochemical techniques are proven to be powerful tools due to their rapid response and simple operation.

The electrochemical oxidation of nitrite offers several advantages with no interference from nitrate ions and from oxygen, which are the major confines in cathodic determination of nitrite. The reduction of NO_2^- yields several products depending on the electrode conditions and the nature of the catalyst employed, and its anodic oxidation is a straight forward reaction, with NO_3^- as the final product. Hence, NO_2^- of determination of has attracted great attention because of it offers several advantages, in particular with no interference. In

contrast, the major limitations of cathodic determination of NO_2^- is due to interference from NO and O_2.

Graphene has a two-dimensional honey-comb lattice discovered by Geim *et al.* in 2004 [17]. It has attracted great attention of both experimental and theoretical scientists in recent years due to its large surface area for applications in various fields such as field-effect transistors [18], sensors [19], electrochemical devices [20], electromechanical resonator [21] polymer nanocomposites [22, 23], batteries [24] and capacitors [25, 26]. All of these properties make it one of the most promising candidates for future nanoelectronics [27] and for widespread applications such as hydrogen storage [28], sensors [29], supercapacitors [30] and nanocomposites [31].

Several methods were reported to synthesize graphene such as chemical vapor deposition [32], micromechanical exfoliation of graphite using peel-off method with Scotch-Tape [33], and epitaxial growth on electrically insulating surface [34]; all of these methods yield graphene nanosheets with good quality [35], which are more suitable for fabrication of graphene-based electronic devices. The other methods including bottom-up synthesis of graphene from organic molecules [36, 37] and the reduction or deoxygenation of graphene oxide (GO) [38-40] are more realistic approaches to produce graphene in gram-level.

One of the most promising approaches to obtain graphene is generated by the oxidation and subsequent exfoliation of graphite to graphene via chemical reduction or thermal treatment [41, 42]. The demerit of the reduction is that the process is very slow and the reductants used are toxic in nature. Moreover graphene nanosheets tend to be restacked due to Vander Waals interactions during the reduction process [43]. The specific surface area of graphene would be decreased due to restacking, which is unfavorable for wide applications of graphene nanosheets. To solve this issue, many approaches have been developed such as stabilizing graphene nanosheets using surfactants, changing the polarity of graphene surfaces by means of grafting polymer chains and decorating graphene surface with metal nanoparticles [44-47] and the abundance of functional groups such as carboxyl, carbonyl, hydroxyl and epoxide on the surfaces and edges of graphene oxide allows for favorable preparation of nanocomposite materials. Recently, incorporating metal nanoparticles on graphene nanosheets provides larger electrochemically active areas for adsorption of biomolecules and efficiently accelerate the electron transfer between electrode and the detection molecules, which could lead to a more rapid and sensitive current response [48].

Decoration of nanoparticles such as Ag [49, 50], Au [51,52], Pt [53], NiO [54], ZnO [55], TiO_2 [56], MnO_2 [57] etc. onto graphene nanosheets have been demonstrated to expose the special features, that can be widely used in variety of applications such as supercapacitors, photocatalysts, Li-ion batteries, electrocatalysis, etc. However assembling Ag nanoparticles on nanostructured materials with electronic and ionic conduction pathways for electrochemical applications still remains a challenge. Here we presented a single step in-situ incorporation of silver nanoparticles onto graphene sheet using aniline as reducing agent in presence of silver nitrite and graphene oxide. The proposed method is simple and effective approach for the incorporation of silver nanoparticles on graphene

and the silver nanoparticles modified graphene with high surface can be utilized for the electrochemical detection of nitrite in food samples.

Experimental Section

Chemicals

Graphite flakes was received from Aldrich Chemicals, Bangalore, India. Other chemicals like silver nitrate, aniline and dimethylformamide (DMF) were purchased from SRL, Pvt Ltd, India. All other chemicals used were received from commercial sources.

Instrumental Methods

Ultraviolet-Visible absorption spectra were recorded for graphene oxide and Ag nanoparticles modified graphene oxide using Shimadzu UV-1800 spectrophotometer, Japan. The XRD patterns of the powdered samples were recorded using X PERT-PRO diffractometer with a Cu Kα Radiation (λ=1.5406 Å), and the crystalline size were estimated using the Scherer equation for some major XRD peaks. The size and morphology of the Ag nanoparticles modified graphene were investigated using SEM XL 30, Philips. SEM micrographs were obtained using a field emission scanning electron microscope equipped with energy dispersive spectrometer (EDS). A single cell compartment with a three electrodes cell setup was used for all electrochemical studies using GAMY 300, USA Potentiostat. A glassy carbon electrode (GCE) electrode (BAS) was used as a working electrode, platinum and Ag wire were used as counter and reference electrode respectively. To modify the GCE a drop cost method was adopted. All solutions were deoxygenated before doing all electrochemical studies.

Experimental Procedure

Synthesis of Graphene Oxide

Graphene Oxide (GO) was synthesized by modified Hummers' method [17] involving three steps. Initially 5 g of graphite powder was taken in a solution of 7.5 mL of conc. H_2SO_4, 2.5 g of $K_2S_2O_8$ and P_2O_5 at 80 °C. 5 g of oxidized graphite powder was placed in cold (0 °C) of conc. H_2SO_4 (115 mL). 15g of $KMnO_4$ was added with stirring, cooled and maintained at < 20 °C. The mixture was then stirred at 35 °C for 2 h, and 230 mL of DI water was added. To terminate the reaction, large amount of DI water, 10% of 12.5 mL H_2O_2 solution, were added over 15 min, and the color has been changed into bright yellow and finally washed with 1 M HCl. After the unexploited graphite in the resulting mixture was removed by centrifugation, as-synthesized graphene oxide (GO) was dispersed into individual sheets in distilled water at a concentration of 0.5 mg/mL with the aid of ultrasound for further use. The Scheme 1 shown explains the synthesis of GO from graphite:

Synthesis of Ag Nanoparticles Modified Graphene Oxide

To prepare AgNP/RGO, an aqueous dispersion of (10 mL) of GO mixed with 200 µL of aniline and 5mL of 0.01 M $AgNO_3$. Then, 15 mL of DMF was added to the reaction mixture and allowed then stirring for 3 hr. The precipitate was collected by centrifugation and washed with water twice and then dried. The Scheme 2 shows the schematic representations for the synthesis of Ag nanoparticles decorated GO.
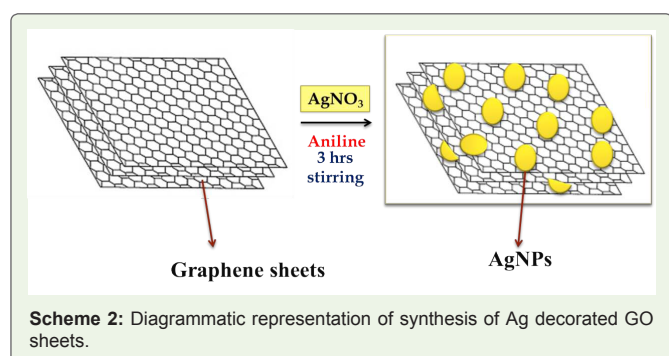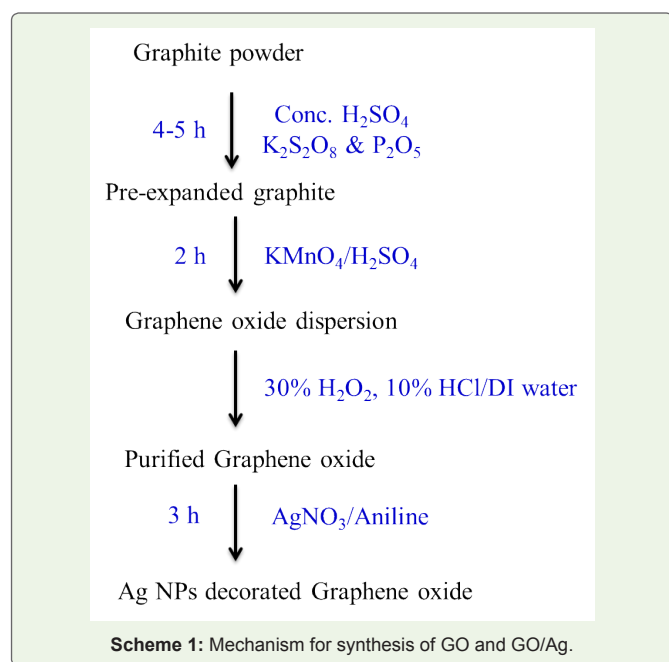
Results and Discussion

UV-Visible Spectral Studies

Figure 1 shows the ultraviolet-visible (UV-Vis) spectrum of graphene oxide (GO) and Ag nanoparticles decorated reduced graphene oxide (RGO/Ag). The UV-visible spectrum of silver nanoparticle decorated graphene oxide gives a characteristic peak at 402 nm indicates the formation of silver nanoparticle and abroad peak at 554 nm arises due to emeraldine form of polyaniline. These results have shown that silver nanoparticles are incorporated onto the surface of reduced graphene oxide during the addition of catalytic amount of aniline. The formation polyaniline during the redox reaction was confirmed from the UV-Visible spectral studies because of the broad peak at 554 nm.

X-ray Diffraction Studies (XRD)

In Figure 2, GO exhibits a strong peak at 10.02° corresponding to the (002) interplanar spacing of 8.2 Å, indicates successful oxidation of graphite by modified Hummers method. In the case of silver nanopar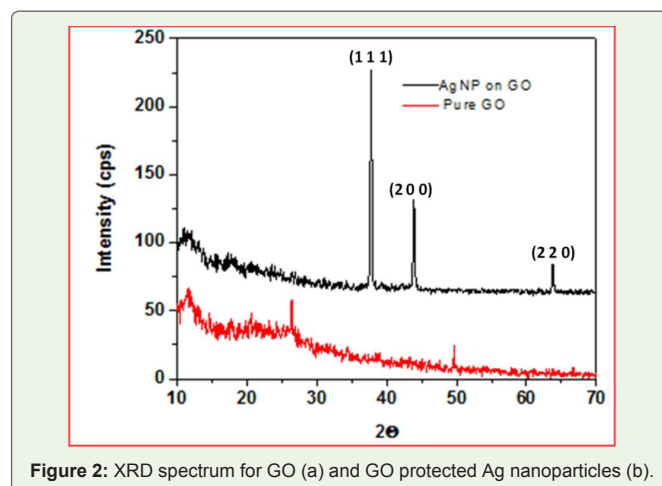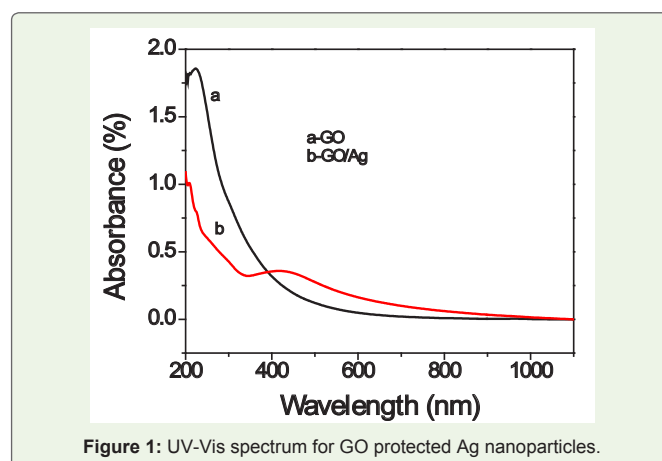ticles modified graphene oxide three major peaks were identified and these peaks are corresponding to (111), (200) and (220) facets of cubic structure of metallic Ag which are observed at 38.3°, 44.5°, and 64.6°, indicates crystalline nature of Ag nanoparticles. The intensity ratio between the (111) and (220) diffraction signals is higher than that shown in the standard file indicates that the Ag nanoparticles are highly crystalline and abundant with (111) facets.

Scanning Electron Microscopy (SEM)

The SEM images of A and B are crumpled and folded graphene layers, bound by vander Waals forces are shown in Fig 3. The Ag nanoparticle/GO composites in C and D formed by the addition of $AgNO_3$ to GO. It is clearly seen that a large amount of Ag nanoparticles (white dots) adsorbed on these GO nanosheets. These Ag nanoparticles on GO sheets are spherical in shape and the sizes ranging from 50 to 60 nm. The energy-dispersive X-ray spectrum (EDAX) of GO and GO-Ag nanocomposites (E and F) indicates the presence of C, O, Ag in the composites, which confirms the formation of Ag nanoparticles on the surfaces of GO sheets.

Electrochemical Behavior of AgNP/RGO

The electrochemical behavior of Ag nanoparticles decorated GO sheets was carried using 0.1 M phosphate buffer solution at pH 7.5

Scheme 1: Mechanism for synthesis of GO and GO/Ag.

Scheme 2: Diagrammatic representation of synthesis of Ag decorated GO sheets.

Figure 1: UV-Vis spectrum for GO protected Ag nanoparticles.

Figure 2: XRD spectrum for GO (a) and GO protected Ag nanoparticles (b).

at a scan rate of 50 mVs⁻¹ and the resulting CV response is shown in Fig 4. A sharp peak at +0.09 V vs. Ag wire is due to the oxidation of Ag (0) to Ag (I). In addition, a reduction peak potential at -0.07 V vs. Ag wire is assigned for the reduction of Ag (I) to Ag (0). These results are consistent with the previously reported literature results [49]. The cyclic voltammogram of AgNP/RGO was recorded at various scan rates under identical conditions. As increase of scan rate, the current responses are increases linearly which is due to the adsorption controlled redox processes in both anodic and cathodic reaction.

Table 1: Comparison of the present work with other reported results.

Electrode	pH	Conc. Range	LOD	Reference
Graphene/poly-cyclodextrin/MWCNTs/GCE	6.0	5–6750 µM	1.65 µM	59
(CoTsPc/PDDA-Gr)n/GCE	5.0	2 – 36 µM	0.084 µM	60
Fe(III)P/MWCNTs/GCE	4.0	1–600 µM	0.5 µM	61
La(OH)3/MWCNT/GCE	6.0	0.55 – 720 µM	0.18 µM	62
Nafion/SLGnPa–TPAb–Mb/GCE	5.0	0.05–2.5 mM	0.01mM	63
p-NiTAPc/GCE	2.0	5×10^{-7}–8×10^{-3} M	1×10^{-7} M	64
SiCe/CPE	-	3×10^{-5}-3.9×10^{-3} M	-	65
CS@PB/GNS–CNS/GCE	2.0	0.002–390 µM	0.001 µM	66
CuTsPc/PLL/GCE	7.0	0.12-12.20 µM	36 nM	67
PEDOT/FePc/MWCNT/SPCF	6.0	-	0.071 µM	68
AgNP/RGO/GCE	7.5	5 – 25 µM	2×10^{-7} M	Present work

Figure 3: SEM image for GO (A & B), GO protected Ag nanoparticles (C & D) and EDX spectrum for GO (F) and GO protected Ag nanoparticles (E).
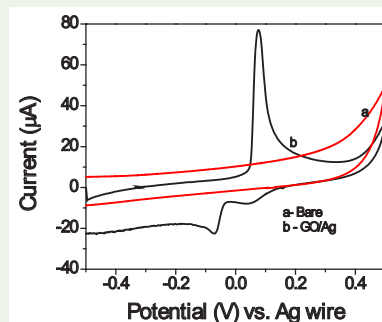

Figure 4: Cyclic voltammogram for bare GCE (a) and GO protected Ag nanoparticles (b) in 0.1 M PBS (pH 7.5) at the scan rate of 50 mVs⁻¹.
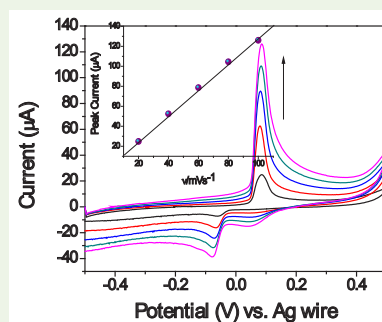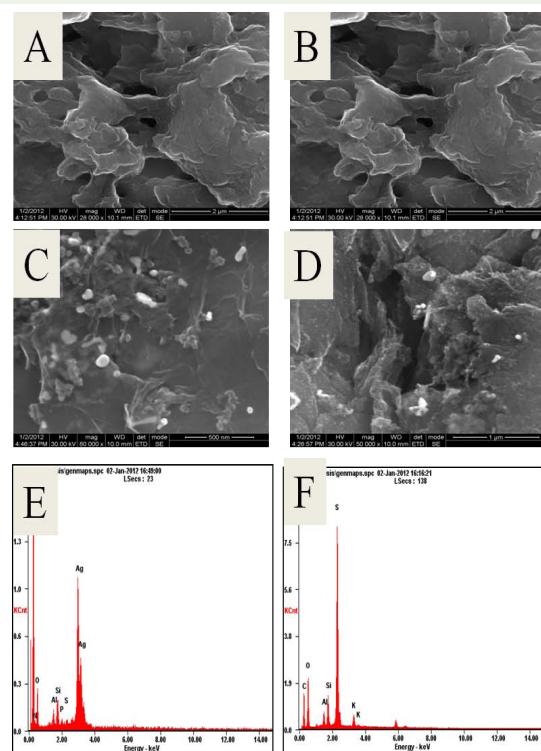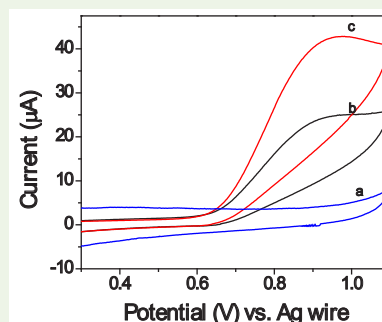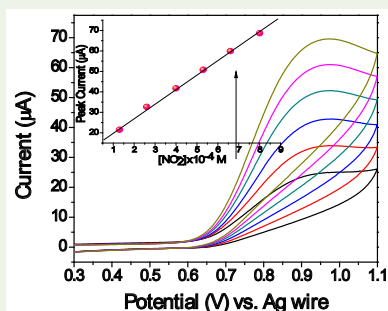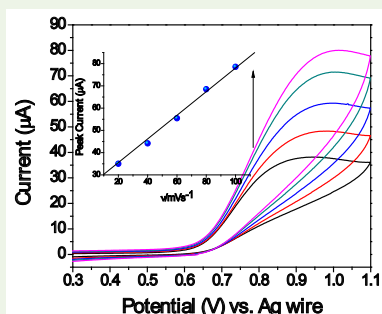

Figure 5: Cyclic voltammogram for GO protected Ag nanoparticles in 0.1 M PBS (pH 7.5) with different scan rates ranging from 20-100 mVs⁻¹. Inset shows the plot of peak current against the scan rate.

Figure 6: Cyclic voltammogram for bare GCE (a), NO_2^-/GCE (b) and GO/Ag/GCE (c) in presence of 1 mM of NO_2^- in 0.1 M PBS (pH 7.5) at the scan rate of 50 mVs⁻¹.

Electrochemical Oxidation of Nitrite using AgNP/RGO modified GCE

The electrochemical oxidation behavior of nitrite (1mM) in both bare GCE and AgNP/RGO modified GCE in 0.1 M phosphate buffer solution (pH 7.5) at a scan rate of 50 mVs⁻¹ are shown in Fig 6. An anodic peak at AgNP/RGO modified GCE was observed at +0.9 V vs. Ag wire. In bare electrode, a less intensity oxidation peak was observed. By comparing the current response for the oxidation of nitrite at bare GCE and the AgNP/RGO modified GCE, an enhanced current response was noted, which implied that AgNP/RGO modified GCE possess a catalytic property that favored the oxidation of nitrite.

Figure 7: Cyclic voltammogram for effect of concentration on electrochemical oxidation of nitrite on GO/Ag modified GCE ranging from 1.3×10^{-4} M to 8×10^{-4} M in 0.1 M PBS (pH 7.5) at the scan rate of 50 mVs^{-1}. Inset shows the plot of peak current against the concentration of nitrite added.

Figure 8: Cyclic voltammogram for effect of scan rate on electrochemical oxidation of nitrite on GO/Ag modified GCE rangng from 20-100 mVs^{-1} in 0.1 M PBS (pH 7.5). Inset shows the plot of peak current against the scan rate.
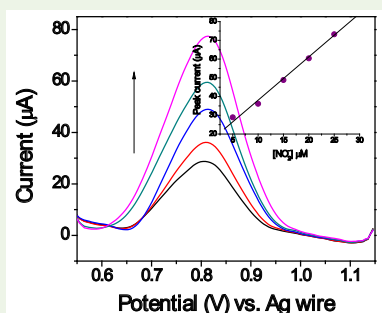
Figure 9: Differential pulse volatammogram for different concentration of nitrite on GO/Ag modified GCE in 0.1M PBS (pH 7.5) containing nitrite ranging from $5 \times 10^{-6} - 25 \times 10^{-6}$ M. Inset shows the plot of peak current against the concentration of nitrite.

The influence of scan rate on electrochemical oxidation of nitrite at AgNP/RGO modified GCE is shown in Fig 7. The catalytic current obtained using AgNP/RGO modified GCE at different concentration of added nitrite is depicted in Fig 8. The peak current increased with respect to increasing concentration and increasing scan rate. Hence the overall process of oxidation of nitrite is diffusion controlled one. In order to determine the concentration of nitrite at trace levels differential pulse voltammetric method was adopted. Fig 9 shows the differential pulse voltammo grams of different concentration of nitrite using AgNP/RGO modified GCE. The inset shows the linear

relation between the oxidation peak current at +0.8 V vs. Ag wire and the concentration of nitrite added each time. The slope for the linear segment is 0.3472, corresponding to different concentrations of nitrite ranging from 5×10^{-6} M to 25×10^{-6} M. The detection limit for nitrite in the above range was found to be 2.6×10^{-7} M. Tab 1 provides detailed information about the comparison data for the present data with all recently reported literature results. To determine the unknown concentration of nitrite present in food samples, a standard addition method was adopted.

Analysis of Nitrite Content in food samples

For the quantitative detection of nitrite in food samples the following subsequent procedure was carried out. Food samples like potato chips were purchased at grocery. About 5 g of the food samples were crushed and homogenized in 20 ml saturated borax solution. To this added 300 ml of hot water (70 – 80 °C) and then the mixture was heated at boiling for 15 min. To precipitate the proteins, 5 ml of 20% zinc acetate was introduced into the reaction mixture. After being cooled to room temperature, the mixture was diluted to a known volume with distilled water (DI) and then filtered. The filtrates were stored at 4 °C in a refrigerator until further use.

The nitrite content in food samples was determined according to the standard addition method. Standard nitrite solutions were added as internal standards after measurement of the sample solution. Thus, the concentration of nitrite in the real sample could be calculated. The differential pulse voltammetry method was utilized for the determination of nitrite present in food samples.

Conclusion

In summary, we have successfully synthesized graphene oxide protected silver nanoparticles using aniline as reducing agent by a single step process. The synthesized nanocomposite was characterized using UV-Vis, SEM, and XRD. The electrochemical behavior of AgNP/RGO was tested and successfully confirmed with cyclic voltammetry and differential pulse voltammetry. A significant increase of peak current was noted for the AgNP/RGO modified GCE which was used as electron transfer mediator because of its high surface area and enhanced oxidation process. The detection limit for oxidation of nitrite was found to be 2.6×10^{-7} M. The resulting sensor displayed an excellent repeatability and long-term stability.

Acknowledgement

References

1. Nielsen M, Larsen LH, Jetten MS, Revsbech NP (2004) Bacterium-based NO$_2^-$ biosensor for environmental applications. Appl Environ Microbiol 70: 6551-8.

2. Silva SM, Mazo LH (1998) Differential Pulse Voltammetric Determination of Nitrite with Gold Ultramicroelectrode. Electroanalysis 10: 1200-1203.

3. Rajesh S, Kanugula AK, Bhargava K, Ilavazhagan G, Kotamraju S. Karunakaran C (2010) Simultaneous electrochemical determination of superoxide anion radical and nitrite using Cu,ZnSOD immobilized on carbon nanotube in polypyrrole matrix. Biosens Bioelectron 26: 689-695.

4. Mirvish SS (1995) Role of N-nitroso compounds (NOC) and N-nitrosation in etiology of gastric, esophageal, nasopharyngeal and bladder cancer and contribution to cancer of known exposures to NOC. Cancer Lett 93: 17-48.

5. Wang P, Mai Z, Dai Z, Li Y, Zou X (2009) Construction of Au nanoparticles on choline chloride modified glassy carbon electrode for sensitive detection of nitrite. Biosens Bioelectron 24: 3242-3247.

6. Almeida MG, Silveira CM, Moura JJ (2007) Biosensing nitrite using the system nitrite redutase/Nafion/methyl viologen--a voltammetric study. Biosens Bioelectron 22: 2485-2492.

7. Geng R, Zhao G, Liu M, Li M (2008) A sandwich structured $SiO^{(2)}$/cytochrome c/$SiO^{(2)}$ on a boron-doped diamond film electrode as an electrochemical nitrite biosensor. Biomaterials 29: 2794-2801.

8. Grau M, Hendgen-Cotta UB, Brouzos P, Drexhage C, Rassaf T, et al. (2007) Recent methodological advances in the analysis of nitrite in the human circulation: nitrite as a biochemical parameter of the L-arginine/NO pathway. J Chromatogr B Analyt Technol Biomed Life Sci 851: 106-123.

9. Tsoulfanidis IA, Tsogas GZ, Giokas DL, Vlessidis AG (2008) Design of a field flow system for the on-line spectrophotometric determination of phosphate, nitrite and nitrate in natural water and wastewater. Microchim Acta 160: 461-469.

10. Helmke SM, Duncan MD (2007) Measurement of the NO metabolites, nitrite and nitrate, in human biological fluids by GC-MS. J Chromatogr B 851: 83-92.

11. Butt SB, Riaz M, Iqbal MZ (2001) Simultaneous determination of nitrite and nitrate by normal phase ion-pair liquid chromatography. Talanta 55: 789-797.

12. Di Matteo V, Esposito E (1997) Methods for the determination of nitrite by high-performance liquid chromatography with electrochemical detection. J Chromatogr A 789: 213-219.

13. Huang K.J, Xie WZ, Zhang HS, Wang H (2008) Ultra-trace level determination of nitrite in human saliva by spectrofluorimetry using 1,3,5,7-tetramethyl-8-(3,4-diaminophenyl)-difluoroboradiaza-s-indacene. Microchim. Acta 161: 201-207.

14. MacArthur PH, Shiva S, Gladwin MT (2007) Measurement of circulating nitrite and S-nitrosothiols by reductive chemiluminescence. J Chromatogr B 851: 93-105.

15. Burakham R, Oshima M, Grudpan K, Motomizu S (2004) Simple flow-injection system for the simultaneous determination of nitrite and nitrate in water samples. Talanta 64: 1259-1265.

16. Szoko E, Tabi T, Halasz AS, Palfi M, Magyar K (2004) High sensitivity analysis of nitrite and nitrate in biological samples by capillary zone electrophoresis with transient isotachophoretic sample stacking. J Chromatogr A 1051: 177-183.

17. Castro Neto AH (2010) The carbon new age. Mater Today 13: 12.

18. Li X, Wang X, Zhang L, Lee S, Dai H (2008) Chemically derived, ultrasmooth graphene nanoribbon semiconductors. Science 319: 1229-1232.

19. Lu CH, Yang HH, Zhu CL, Chen X, Chen GN (2009) A graphene platform for sensing biomolecules. Angew. Chem. Int. Ed Engl 48: 4785-4787.

20. Schedin F, Geim AK, Morozov SV,. Hill EW, Blake P, et al., (2007) Detection of individual gas molecules adsorbed on graphene. Nat. Mater 6:652-655.

21. Bunch JS, Zande AM, Verbridge SS, Frank IW, Tanenbaum DM, et al. (2007) Electromechanical Resonators from Graphene Sheets. Science 315: 490-493.

22. Ramanathan T, Abdala AA, Stankovich S, Dikin DA, Herrera-Alonso M, et al. (2008) Functionalized graphene sheets for polymer nanocomposites. Nat Nanotechnol 3: 327-331.

23. Yoon JH, Shanmugharaj AM, Choi WS, Ryu SH (2011) ICCM18: The 18th International Conference on Composite Materials. 18th International Conference On Composite Materials, South Korea.

24. Yoo E, Kim J, Hosono E, Zhou HS, Kudo T, Honma I (2008) Large reversible Li storage of graphene nanosheet families for use in rechargeable lithium ion batteries. Nano Lett 8: 2277-2282.

25. Stoller MD, Park S, Zhu Y, An J, Ruoff RS (2008) Graphene-based ultracapacitors. Nano Lett 8: 3498-3502.

26. Qian Y, Lu SB, Gao F (2011) Preparation of MnO_2/graphene composite as electrode material for supercapacitors. J Mater Sci 46: 3517.

27. Areshkin DA, White CT (2007) Building blocks for integrated graphene circuits. Nano Lett 7: 3253-3259.

28. Zhou Y, Bao Q, Tang LAL, Zhong Y, Loh KP (2009)Hydrothermal Dehydration for the "Green" Reduction of Exfoliated Graphene Oxide to Graphene and Demonstration of Tunable Optical Limiting Properties. Chem Mater 21: 2950-2956

29. Qian Y, (2012) Synthesis of Cuprous Oxide (Cu_2O) Nanoparticles/Graphene Composite with an Excellent Electrocatalytic Activity Towards Glucose. Int J Electrochem Sci7: 10063-10073.

30. Wang HL, Liang YY, Mirfakhrai Chen TZ, Casalongue HS, et al. (2011) Advanced Asymmetrical Supercapacitors Based on Graphene Hybrid Materials. Nano Res 4: 729-736.

31. Zhao X, Zhang QH, Chen DJ (2010) Enhanced Mechanical Properties of Graphene-Based Poly(vinyl alcohol) Composites. Macromol 43: 2357-2363.

32. Park S, Ruoff RS (2009) Chemical methods for the production of graphenes. Nat Nanotechnol 4: 217-.224

33. Kim FS, Zhao Y, Jang H., Lee SY, Kim JM, et al. (2009) Large-scale pattern growth of graphene films for stretchable transparent electrodes. Nature, 457 :706-710.

34. Lu X, Yu M, Huang H Ruoff RS (1999) Tailoring graphite with the goal ofachieving single sheets. Nanotechnology10: 269-272.

35. Bae S, Kim H, Lee Y, Xu XF, Park JS, et al. (2010) Roll-to-roll production of 30-inch graphene films for transparent electrodes. Nat Nanotechnol 5: 574-578.

36. Wu J, Pisula W, Müllen K (2007) Graphenes as potential material for electronics. Chem Rev 107: 718-747.

37. Kuang Q, Xie SY, Jiang ZY, Zhang XH, Xie ZX, et al. (2004) Low temperature solvothermal synthesis of crumpled carbon nanosheets. Carbon 42: 1737-1741.

38. S. Stankovich (2007) Synthesis of graphene-based nanosheets via chemical reduction of exfoliated graphite oxide Carbon 45: 1558-1565.

39. Dreyer DR, Park S, Bielawski CW, Ruoff RS (2010) The chemistry of graphene oxide. Chem Soc Rev 39: 228-240.

40. Zu SZ, Han BH (2009) Aqueous Dispersion of Graphene Sheets Stabilized by Pluronic Copolymers: Formation of Supramolecular Hydrogel. J Phys Chem C 113: 13651-13657.

41. Tung VC, Allen MJ, Yang Y, R.B. Kaner (2008) High-throughput solution processing of large-scale grapheme. Nat Nanotechnol 4: 25-29.

42. Schniepp HC, Li JL, McAllister MJ, Sai H, Herrera-Alonso M et al. (2006) Functionalized single graphene sheets derived from splitting graphite oxide. J Phys Chem B 110: 8535-8539.

43. Liang YY, Wu DQ, Feng XL, Mullen K (2009) Dispersion of Graphene Sheets in Organic Solvent Supported by Ionic Interactions. Adv Mater 21: 1679-1683.

44. Qian Y, Wang CY, Le ZG (2011) Appl Surf Sci 256: 10758.

45. Fang M, Wang KG, Lu HB, Yang YL, Nutt S (2010) Single-layer graphene nanosheets with controlled grafting of polymer chains. J Mater Chem 20: 1982-1992.

46. He H, Gao C (2010) General Approach to Individually Dispersed, Highly Soluble, and Conductive Graphene Nanosheets Functionalized by Nitrene Chemistry. Chem Mater 22: 5054-5064.

47. Zhang FY, Wang ZH, Zhang YZ, Zheng ZX, Wang CM, *et al.,* (2010) Int. J. Electrochem Sci 7: 1968.

48. Pumera M, (2010) Graphene-based nanomaterials and their electrochemistry. Chem Soc Rev 39: 4146-4157.

49. Xu C, Wang X (2009) Fabrication of flexible metal-nanoparticle films using graphene oxide sheets as substrates. Small 5: 2212-2217.

50. Lu WB, Chang GH, Luo YL, Liao F, Sun XP (2011) Method for effective immobilization of Ag nanoparticles/graphene oxide composites on single-stranded DNA modified gold electrode for enzymeless H2O2 detection. J Mater Sci 46: 5260-5266.

51. Yan SH, Zhang SC, Lin Y, Liu GR (2011) Electrocatalytic Performance of Gold Nanoparticles Supported on Activated Carbon for Methanol Oxidation in Alkaline Solution. J Phys Chem C 115: 6986-6993.

52. Zhang Z, Wu Y (2010) Investigation of the NaBH4-induced aggregation of Au nanoparticles. Langmuir 26: 9214-9223.

53. Li YJ, Gao W, Ci LJ, Wang CM (2010) Catalytic performance of Pt nanoparticles on reduced graphene oxide for methanol electro-oxidation. Carbon 48: 1124-1130.

54. Ji ZY, Wu JL, Shen XP, Zhou H, Xi HT (2011) Preparation and characterization of graphene/NiO nanocomposites. J Mater Sci 46: 1190-1195.

55. Wu J, Shen X, Jiang L, Wang K, Chen K (2010) Solvothermal synthesis and characterization of sandwich-like graphene/ZnO nanocomposites. Appl Surf Sci 256: 2826-2830.

56. Wang D, Choi D, Li J, Yang Z, Nie Z et al. (2009) Self-assembled TiO2-graphene hybrid nanostructures for enhanced Li-ion insertion. ACS Nano 3: 907-914.

57. Chen S, Zhu J, Wu X, Han Q, Wang X (2009) Graphene oxide--MnO2 nanocomposites for supercapacitors. ACS Nano 4: 2822-2830.